

Short Gamma Ray Bursts: a bimodal origin?

R. Salvaterra¹, A. Cerutti¹, G. Chincarini^{1,2}, M. Colpi¹, C. Guidorzi^{1,2}, & P. Romano^{1,2}

¹ *Dipartimento di Fisica G. Occhialini, Università degli Studi di Milano Bicocca, Piazza della Scienza 3, I-20126 Milano, Italy*

² *INAF, Osservatorio Astronomico di Brera, via E. Bianchi 46, I-23807 Merate (LC), Italy*

4 November 2018

ABSTRACT

Short–hard Gamma Ray Bursts (SGRBs) are currently thought to arise from gravitational wave driven coalescences of double neutron star systems forming either in the field or dynamically in globular clusters. For both channels we fit the peak flux distribution of BATSE SGRBs to derive the local burst formation rate and luminosity function. We then compare the resulting redshift distribution with *Swift* 2-year data, showing that both formation channels are needed in order to reproduce the observations. Double neutron stars forming in globular clusters are found to dominate the distribution at $z \lesssim 0.3$, whereas the field population from primordial binaries can account for the high- z SGRBs. This result is not in contradiction with the observed host galaxy type of SGRBs.

Key words: gamma-ray: burst – stars: formation – cosmology: observations.

1 INTRODUCTION

The afterglows of several Short Gamma Ray Bursts (SGRBs) have recently been localised on the sky with *Swift* (Gehrels et al. 2004) and *HETE-II* (Lamb et al. 2004), allowing for the determination of their redshift and host galaxy (Nakar 2007; Berger et al. 2007a, and references therein). For SGRBs, the data give mean redshift $z \sim 0.6$, and early as well as late type galaxy hosts.

The current idea on the nature of the SGRBs is that they arise from gravitational wave driven mergers of neutron star–neutron star and/or neutron star–black hole binaries (Belczynski et al. 2006; Nakar 2007). Double neutron star binaries (DNSs) are observed in the field of the Milky Way and in globular clusters, so they can form through two different channels: (i) evolution of primordial massive star binaries, formed in the galactic field (field scenario; Narayan, Paczynski & Piran 1992), and (ii) dynamical formation^{*}, through three-body interactions in globular clusters (GCs) involving the exchange of a light star companion of a neutron star with an incoming isolated neutron star (GC scenario; Grindlay, Portegies Zwart & Mc Millan 2006).

In this Letter, we derive the local SGRB formation rate and luminosity function by fitting the peak flux distribution of the large sample of BATSE SGRBs (Paciesas et al. 1999) exploring both formation scenarios. We compare the model results with the redshift distribution of the sample of *Swift* SGRBs in the first two years of operation, with the aim

of disentangling the relative importance of the two SGRB populations at different cosmic epochs.

2 SGRB FORMATION MODELS

In this section we compute the intrinsic formation history of SGRBs for the two scenarios: the field scenario, where DNSs correlate with the overall star formation and the dynamical one inside GCs.

In the field scenario, the intrinsic formation rate, defined as the number of bursts per unit time and unit comoving volume at redshift z , $\Psi_{\text{SGRB}}(z)$, is given by the convolution of the massive star binary formation rate and a delay time distribution function $f_{\text{F}}(t)$. The delay is the time interval between the formation of the massive star binary and the merging of the DNSs due to gravitational wave emission. The formation rate is assumed to be proportional to the cosmic star formation rate, $\dot{\rho}_{\star}$, parametrized as in Hopkins & Beacom (2006). $\Psi_{\text{SGRB}}(z)$ is given by

$$\Psi_{\text{SGRB}}(z) \propto \int_z^{\infty} dz' \frac{dt}{dz'}(z') \dot{\rho}_{\star}(z') f_{\text{F}}[t(z) - t(z')], \quad (1)$$

where $t(z)$ is the age of the Universe at redshift z . For the delay time distribution function $f_{\text{F}}(t)$, we adopt the following simple expression: $f_{\text{F}}(t) \propto 1/t$, as suggested from an updated analysis of double compact object mergers performed using population synthesis methods (Portegies Zwart & Yungelson 1998, Schneider et al. 2001, Belczynski et al. 2006, O’Shaughnessy et al. 2008). Moreover this form seems to be supported by the distribution of the orbital parameters of six DNSs observed in our Galaxy (Champion et al.

^{*} Formation of primordial DNSs may not be efficient in globular clusters (Ivanova et al 2008).

2004). Characteristic delay times vary from ~ 20 Myr to ~ 10 Gyr.

Similarly, in the GC scenario, $\Psi_{\text{SGRB}}(z)$ is given by convolution of the GC formation rate, $\dot{\rho}_{\text{GC}}(z)$, with a delay function $f_{\text{GC}}(t)$:

$$\Psi_{\text{SGRB}}(z) \propto \int_z^\infty dz' \frac{dt}{dz'}(z') \dot{\rho}_{\text{GC}}(z') f_{\text{GC}}[t(z) - t(z')]. \quad (2)$$

Hopman et al. (2006) considered $\dot{\rho}_{\text{GC}}$ proportional to the observed star formation rate. Here we explore here three different possibilities for $\dot{\rho}_{\text{GC}}$:

- model GC1: constant between $z = 3$ and $z = 5$ and null outside this interval, as suggested from studies of GC formation in the cosmological context (Kravtsov & Gnedin 2005);
- model GC2: obtained from the GC age distribution of the spiral galaxy M31 (Fan et al. 2006);
- model GC3: obtained from the GC age distribution of the elliptical galaxy M87 (Cohen, Blakeslee & Ryzhov 1998).

For a comparison with Hopman et al. (2006) we explore a model where $\dot{\rho}_{\text{GC}}$ follows the star formation rate, here computed following Hopkins & Beacom (2006), and referred as model GC4.

As regard to the function f_{GC} , the delay time is the sum of the interval between the formation of the GC and the dynamical formation of the DNS, plus the DNS coalescence time due to gravitational wave emission. The first time interval is set equal to the core-collapse time since, only after the GC has experienced core-collapse, the rate of DNS formation due to gravitational encounters becomes relevant (Hopman et al. 2006). So the delay function $f_{\text{GC}}(t)$ is the convolution of the core-collapse time distribution and the gravitational wave coalescence time distribution. Following Hopman et al. (2006), the former is computed from the compilation of the half-mass relaxation times and concentrations of the observed GCs in our Galaxy by Harris (1996)[†] combined with the core-collapse time distribution from Quinlan (1996).

The latter is obtained from three-body simulations of encounters between single neutron stars and target binaries in GCs. The resulting distribution of eccentricities and orbital periods of the simulated DNS binaries yields a delay function $\propto t^{-1.06}$ (Cerutti 2007) in close agreement with Hopman et al. (2006). Characteristic delay times are longer than in the field case (> 3 Gyr), and determined mainly by the extent of the core-collapse time.

3 THE SGRB LUMINOSITY FUNCTION

For a comparison with data, we here compute the observed distribution of SGRBs for the different DNS formation scenarios.

The observed photon flux, P , in the energy band $E_{\text{min}} < E < E_{\text{max}}$, emitted by an isotropically radiating source at redshift z is

[†] We implicitly assume that the properties of GCs in Harris's catalogue are representative of the population of GCs also in external galaxies.

Model	k_{SGRB} [Gpc ⁻³ yr ⁻¹]	$L_0/10^{50}$ erg s ⁻¹	β	χ_r^2
field	12.7±4.6	1.16±0.01	1.41±0.22	1.1
GC1	23.9±2.5	8.26±0.01	2.68±0.31	1.2
GC2	90.2±11.6	3.22±0.01	2.72±0.37	1.2
GC3	22.3±2.5	8.93±0.02	2.76±0.37	1.3
GC4	37.6±2.3	6.81±0.01	2.80±0.29	1.3

Table 1. Best-fit parameters for the different DNS scenarios. Errors are at 1σ level. The value of k_{SGRB} is obtained in the hypothesis that the emission is isotropic (see Nakar 2007 for a discussion of the beaming factor).

$$P = \frac{(1+z) \int_{(1+z)E_{\text{min}}}^{(1+z)E_{\text{max}}} S(E) dE}{4\pi d_L^2(z)}, \quad (3)$$

where $S(E)$ is the differential rest-frame photon luminosity of the source, and $d_L(z)$ is the luminosity distance. To describe the typical burst spectrum we adopt a single power-law with an exponential cut-off with index -0.58 and rest-frame break energy $E_b \sim 400$ keV (Ghirlanda, Ghisellini & Celotti 2004) where we assume a mean redshift of ~ 0.6 for SGRBs. We define the isotropic equivalent intrinsic burst luminosity as $L = \int_{30 \text{ keV}}^{2000 \text{ keV}} S(E) E dE$.

Given a normalized SGRB luminosity function, $\phi(L)$, the observed rate of bursts with peak flux between P_1 and P_2 is

$$\begin{aligned} \frac{dN}{dt}(P_1 < P < P_2) &= \int_0^\infty dz \frac{dV(z)}{dz} \frac{\Delta\Omega_s}{4\pi} \frac{k_{\text{SGRB}} \Psi_{\text{SGRB}}(z)}{1+z} \\ &\times \int_{L(P_1, z)}^{L(P_2, z)} dL' \phi(L'), \end{aligned} \quad (4)$$

where $dV(z)/dz = 4\pi c d_L^2(z)/[H(z)(1+z)^2]$ is the comoving volume element[‡], and $H(z) = H_0[\Omega_M(1+z)^3 + \Omega_\Lambda + (1 - \Omega_M - \Omega_\Lambda)(1+z)^2]^{1/2}$. $\Delta\Omega_s$ is the solid angle covered on the sky by the survey, and the factor $(1+z)^{-1}$ accounts for cosmological time dilation. $\Psi_{\text{SGRB}}(z)$ is the comoving burst formation rate normalized to unity at $z = 0$ as computed in Section 2 and k_{SGRB} is the SGRB formation rate at $z = 0$.

In this work, we assume a luminosity function described by a double power-law

$$\phi(L) \propto \begin{cases} (L/L_0)^{-\alpha} & \text{for } L < L_0 \\ (L/L_0)^{-\beta} & \text{for } L > L_0, \end{cases} \quad (5)$$

with $\alpha = 1.6$ (Schmidt 2001) in order to reduce the number of model free parameters. The power index β is a free parameter of the model. The values obtained by fitting BATSE data are listed in Table 1.

We fit the differential photon flux distribution of SGRBs with $T_{90} < 2$ s detected by BATSE in the 50-300 keV band (Paciesas et al. 1999). We consider the observed photon fluxes in the 64 ms timing window, restrict our fitting procedure to $P_{64} \geq 1 \text{ ph s}^{-1} \text{ cm}^{-2}$ for which the detector response

[‡] We adopted the concordance model values for the cosmological parameters: $h = 0.7$, $\Omega_M = 0.3$, and $\Omega_\Lambda = 0.7$.

SGRB	T_{90} [s]	$P(64\text{ms})$ [ph s $^{-1}$ cm $^{-2}$]	z	Used	References
050202	0.27	4.0 ± 0.4		Y	1
050509B	0.073	1.3 ± 0.2	0.226	N	2,3,4,5
050724	$\sim 3^*$	11.0 ± 0.8	0.257	Y	6,7,8,9,10,1,5
050813	0.45	2.1 ± 0.21	0.72 or 1.8	Y	11,1,5
050906	0.258	1.7 ± 0.3		N	1
050925	0.07	10.8 ± 1.0		Y	5
051105A	0.093	2.7 ± 0.5		Y	1
051210	1.3	1.0 ± 0.2		N	12,1,13,5
051221A	1.4	40.7 ± 1.5	0.547	Y	14,1,13,5
060313	0.74	30.9 ± 0.9		Y	15,1,16,13,5
060502B	0.131	3.4 ± 0.2	0.287	Y	17,1,13,5
060801	0.49	2.1 ± 0.2	1.1304	Y	13
061006	$\sim 0.42^*$	12.9 ± 0.4	0.4377	Y	13
061201	0.76	8.0 ± 1.0	0.111	Y	5
061210	$\sim 0.19^*$	38.5 ± 1.1	0.41	Y	18
061217	0.21	2.0 ± 0.2	0.827	Y	5
070209	0.09	2.8 ± 0.4		Y	19

Table 2. *Swift* SGRBs. T_{90} from Sakamoto et al. (2007) apart from the SGRBs denoted with * where we refer to the duration of the main pulse. In the column ‘Used’, we indicate with Y (N) the burst that we (don’t) use in our analysis. References (1), (3), (5), (9), (10), (12), (13), (15), (16), (19) are on the short nature of the burst, whereas others refer to host and/or redshift determination. References: (1) Donaghy et al. (2006), (2) Gehrels et al. (2005), (3) Lee et al. (2005), (4) Bloom et al. (2006b), (5) Berger (2007), (6) Barthelmy et al. (2005), (7) Berger et al. (2005), (8) Prochaska et al. (2006), (9) Campana et al. (2006), (10) Grupe et al. (2006), (11) Berger (2005), (12) La Parola et al. (2006), (13) Berger et al. (2007a), (14) Soderberg et al. (2006), (15) Roming et al. (2006), (16) Postigo et al. (2006), (17) Bloom et al. (2006a), (18) Berger (2006), (19) Sato et al. (2007)

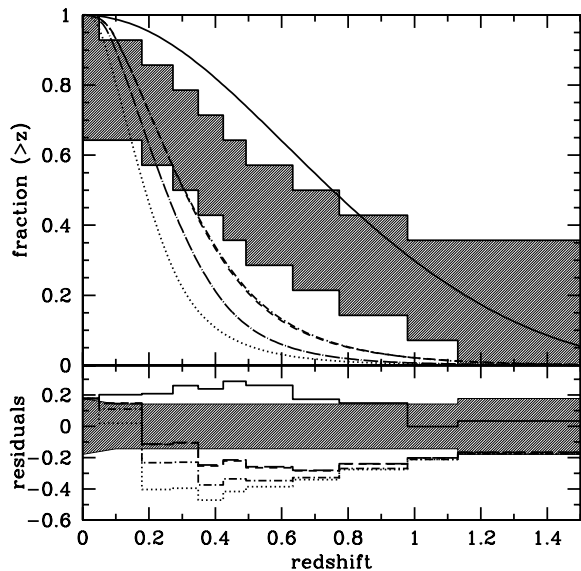


Figure 1. Shaded area: observed cumulative redshift distribution of *Swift* SGRBs with $P_{64} > 2$ ph s $^{-1}$ cm $^{-2}$, taking into account uncertainties due the lack of a secure redshift determination for some SGRBs. Model results are overplotted for different DNS formation channels: solid line refers to field scenario, dot-short dashed to GC1, dotted to GC2, short dashed to GC3, and dot-long dashed to GC4. In the bottom panel we plot the residuals to enhance the difference between the model results and the observed distribution.

is efficient, and adopt a effective field of view for BATSE, defined as $(\Delta\Omega_s/4\pi)t_{\text{obs}}$, of 1.8 yr. The best fit parameters are given in Table 1. We obtain a reasonable fit to BATSE data in all formation scenarios by adjusting the free parameters of the model. In this work we neglect the presence of a possible contamination from Soft Gamma-Ray Repeaters at low redshifts (Hurley et al. 2005) which is still difficult to quantify (see Chapman et al. 2008).

We then compute the expected SGRB rate in the 15–150 keV band of *Swift* adopting a field of view $\Delta\Omega_s = 1.4$ sr, and a 2-year mission. For a correct comparison between model results and *Swift* data, we calculate the photon peak flux for *Swift* SGRBs in a timing window similar to the one used on BATSE. Peak fluxes of *Swift* GRBs are calculated on different integration times, spanning from 64 to 448 ms, in order to match common significance criteria and compatibly with the duration of the peak itself. These are consistent within uncertainties with the corresponding values integrated on a fixed 64-ms window. This makes the comparison with BATSE well grounded. The photon fluxes P_{64} for the SGRBs observed with *Swift* are collected in Table 2.

The few *Swift* detections do not allow to construct a reliable differential peak flux distribution. However, we expect $\sim 9 - 10$ SGRBs per year with $P_{64} \geq 2$ ph s $^{-1}$ cm $^{-2}$ for all our models, in agreement with the 7 SGRBs per year detected by *Swift* at the same flux limit. Note that this is a lower limit since we do not consider here SGRBs that are identified in the ground analysis (e.g., GRB 051114) and those long GRBs that could be tentatively ascribed to the short category (e.g., GRB 060614, and 060505). Lowering the *Swift* photon flux threshold down to 1 ph s $^{-1}$ cm $^{-2}$, the expected SGRB detections largely exceed the number of identified SGRBs. This fact may be related to a different

energy band and trigger procedure of *Swift* and BATSE. We thus choose the threshold of $2 \text{ ph s}^{-1} \text{ cm}^{-2}$ as measured in a 64 ms timing window as reliable detection limit for *Swift*.

4 REDSHIFT DISTRIBUTION

In Table 2 we list all SGRBs detected by *Swift* until march 2007 with, when present, the redshift. We note that GRB 050509B, 050906, and 051210 are not included in our analysis being their photon flux in the 64 ms timing window below the threshold limit we adopted. To be conservative, we assume that GRB 050813 lies at $z = 0.72$ instead of $z = 1.8$. The shaded area in Fig. 1 accounts for the observed cumulative z -distribution including the uncertainties due the lack of a secure redshift determination for some SGRBs. Model results computed for the different DNS formation channels are shown in Fig. 1: solid line refers to the field scenario, dot-short dashed for GC1, dotted for GC2, dashed for GC3, and dot-long dashed for GC4. For the field scenario our fit is close to model (ii) of Guetta & Piran (2007). For the GC scenario, we note that in spite of the different assumptions of the GC formation rate, the expected SGRB z -distributions are not remarkably different. The key result is that DNSs from dynamical interactions in GC may account only for the lowest redshift SGRBs, i.e. $z < 0.2 - 0.3$. We find that only 4–12% of SGRBs in GC should lie above $z = 0.6$ [§]. This result is expected owing to the longer delay times in the formation and coalescence of DNSs in GCs relative to the field. Field DNSs form earlier and for this reason they can account for the SGRB distribution above $z = 0.8$. Instead, the field scenario results inconsistent with *Swift* data below this redshift. This appears to be little affected by our choice of α in the luminosity function, although the best-fit parameters in Table 1 may vary significantly.

Hopman et al. (2006) first noticed that SGRBs at low- z may come from dynamical formation of DNSs in GCs and possibly ascribed all the SGRBs in the *Swift* catalogue to this formation channels. We find here that *Swift* 2-year data seem favour a bimodal origin of SGRBs: the nearby, low- z bursts resulting preferentially from dynamical forming DNSs, whereas distant, high- z bursts resulting from the coalescence of primordial DNSs following the cosmic star formation history.

Although current uncertainties are very large and the data sample poor, we can try to quantify the relative weight of the two channels. In order to reproduce the observed limits on the redshift distribution of SGRBs, almost 30%–70% of SGRBs detected by *Swift* should come from primordial NS-NS binary mergers if models GC1 or GC3 are considered. For model GC2 this fraction increases up to 50–80%. We can rewrite these results in terms of the ratio between the intrinsic formation rates at $z = 0$ in the two channels, i.e. $\eta = k_{\text{SGRB,F}}/k_{\text{SGRB,GC}}$. We find that $\eta = 0.22 - 1.24$ for model GC1 and GC3, and $\eta = 0.14 - 0.56$ for GC2. A large sample of SGRB detection and host identifications are needed in order to confirm these findings.

[§] NS-NS binaries in young and dense star clusters may form dynamically and enhance the rate of dynamical channel, at high redshifts in star forming galaxies.

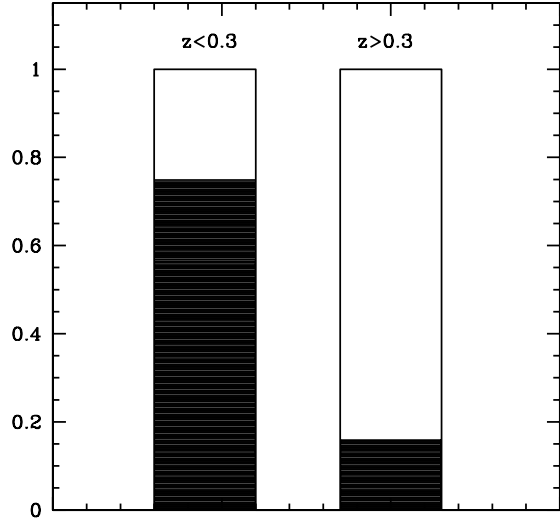


Figure 2. Fraction of SGRBs hosted in early-type (shaded area) and late-type (white area) galaxies below $z = 0.3$ and above.

5 CONCLUSIONS

We have shown that current *Swift* data seem to point towards a dual nature of SGRB formation: low- z SGRBs may arise from the coalescence of DNSs forming in GCs through dynamical collisions, whereas high- z bursts can represent the end-result of DNS mergers born in the field from primordial massive binary stars. A way to falsify this bimodality is by considering the correlation between SGRBs and the host galaxy type (Gam-Yam et al. 2005; Zheng & Ramirez-Ruiz 2007; Berger et al. 2007b; Shin & Berger 2007). We expect that SGRBs from the GC channel should be found preferentially in early type galaxies where the bulk of GCs resides, although we can not completely exclude a few in spirals. On the contrary, field SGRBs can be hosted in both early and late type galaxies given the wide distribution of delay times (Section 2). Since the dynamical channel produces SGRBs at low- z , we expect to find an excess of SGRBs in early type galaxies below $z < 0.3$. At present it is still premature to exploit this issue in a statistically meaningful manner and we may just confine ourselves to the analysis of SGRBs in the current limited sample. Up to now, four SGRBs have been localised in early-type galaxies (GRB 050509B, 050724, 050813, and 060502B), whereas six have secure late-type hosts (GRB 051221A, 060801, 061006, 061210, and 061217, Berger 2007; *HETE-II* GRB 050709 at $z = 0.161$; Fox et al. 2005; Covino et al. 2006). Fig. 2 shows the fraction of SGRB hosts in early (shaded area) and late (white area) below $z = 0.3$ and above, respectively. We note indeed that low- z SGRBs are associated preferentially to early-type galaxies while the high- z ones are located in late-type. The large offset of GRB 050509B and 060502B may support further the association of these SGRBs with DNSs formed dynamically in GCs.

REFERENCES

- Barthelmy S. D. et al., 2005, *Nature*, 438, 994
- Belczynski K., Perna R., Bulik T., Kalogera V., Ivanova N., Lamb D. Q., 2006, *ApJ*, 648, 1110
- Berger E., 2005, GCN 3801
- Berger E., 2006, GCN 5952
- Berger E., 2007, *ApJ* submitted, astro-ph/0702694
- Berger E. et al., 2005, *Nature*, 438, 988
- Berger E. et al., 2007a, *ApJ*, 664, 1000
- Berger E., Shin, M.-S., Mulchaey J. S., Jeltama T. E., 2007b, *ApJ*, 660, 496
- Bloom J. S. et al., 2006a, GCN 5238
- Bloom J. S. et al., 2006b, *ApJ*, 638, 354
- Campana S. et al., 2006, *A&A*, 454, 113
- Cerutti A., 2007, Degree Thesis
- Champion D.J., Lorimer D R., McLaughlin M.A., Cordes J.M., Arzoumanian Z., Weisberg J.M., Taylor J.H., 2004, *MNRAS*, 350, L61
- Chapman R., Priddey R.S., Tanvir N.R., 2008, *MNRAS*, submitted, arXiv:0802.0008
- Cohen J.G., Blakelee J.P., & Ryzhov A., 1998, *ApJ*, 496, 808
- Covino S. et al., 2006, *A&A*, 447, L5
- Donaghy T. Q. et al., 2006, *ApJ* submitted, astro-ph/0605570
- Fan Z., Ma, J., de Grijs R., Yang Y., Zhou X., 2006, *MNRAS*, 371, 1648
- Fox D.B. et al., 2005, *Nature*, 437, 845
- Gal-Yam A. et al., 2005, arXiv:astro-ph/0509891
- Gehrels N. et al., 2004, *ApJ*, 611, 1005
- Gehrels N. et al., 2005, *Nature*, 437, 851
- Ghirlanda G., Ghisellini, G. & Celotti, A., 2004, *A&A*, 422, L55
- Grindlay J., Portegies Zwart S., McMillan S., 2006, *NatPh*, 2, 116
- Grupe D. et al., 2006, *ApJ*, 653, 462
- Guetta D. & Piran T., 2006, *A&A*, 453, 823
- Kravtsov A. V. & Gnedin O. Y., 2005, *ApJ*, 623, 650
- Harris W.E., 1996, *AJ*, 112, 1487
- Hopkins A. M. & Beacom J. F., 2006, *ApJ*, 651, 142
- Hopman C., Guetta D., Waxman E., Portegies Zwart S., 2006, *ApJ*, 643, 91
- Hurley K. et al., 2005, *Nature*, 434, 1098
- Ivanova N., Heinke C.O., Rasio F.A., Belczynski K., Fregeau J.M., 2008 *MNRAS* in press, arXiv:0706.4096
- Lamb D. et al., 2004, *NewAR*, 48, 423
- La Parola V. et al., 2006, *A&A*, 454, 753
- Lee W. H., Ramirez-Ruiz E., Granot J., 2005, *ApJ*, 630, L165
- Nakar E., 2007, *PhR*, 442, 166
- Narayan R., Paczynski B., & Piran T., 1992, *ApJ*, 395, L8
- O'Shaughnessy R., Belczynski K., Kalogera V., 2008, *ApJ*, 675, 566
- Paciesas W. S. et al., *ApJS*, 122, 465
- Portegies Zwart S.F. & Yungelson L. R., 1998, *A&A*, 332, 173
- Postigo A.d.U. et al., 2006, *ApJ*, 648, L83
- Prochaska J. X. et al., 2006, *ApJ*, 642, 989
- Quilan G.D., 1996, *NewA*, 1, 255
- Roming P. W. A. et al., 2006, *ApJ*, 651, 985
- Sakamoto T. et al., 2007, to be published on *ApJS*, arXiv:0707.4626
- Sato G. et al., 2007, GCN 6086
- Schmidt M., 2001, *ApJ*, 559, L79
- Schneider R., Ferrari V., Matarrese S., Portegies Zwart S.F., 2001, *MNRAS*, 324, 797
- Shin M.-S. & Berger E., 2007, *ApJ*, 660, 1146
- Soderberg A. M. et al., 2006, *ApJ*, 650, 261
- Zheng Z. & Ramirez-Ruiz E., 2007, *ApJ*, 665, 1220